



ulm university

universität
uulm

Radar Sensors for Autonomous Driving: Modulation Schemes and Interference Mitigation

Fabian Roos, Jonathan Bechter, Christina Knill, Benedikt Schweizer, and Christian Waldschmidt

© 2019 IEEE. Personal use of this material is permitted. Permission from IEEE must be obtained for all other uses, in any current or future media, including reprinting/republishing this material for advertising or promotional purposes, creating new collective works, for resale or redistribution to servers or lists, or reuse of any copyrighted component of this work in other works.

DOI: 10.1109/MMM.2019.2922120

Radar Sensors for Autonomous Driving: Modulation Schemes and Interference Mitigation

Fabian Roos, Jonathan Bechter, Christina Knill, Benedikt Schweizer, and Christian Waldschmidt

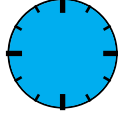
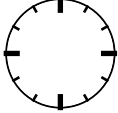
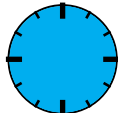
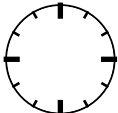
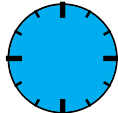
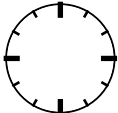
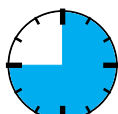
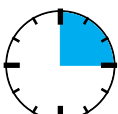
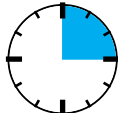
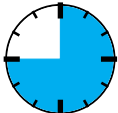
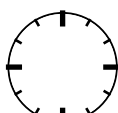
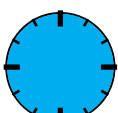
1 Introduction

The topic of autonomous driving currently draws much media attention, and automobile manufacturers and component suppliers are working on the realisation of autonomous vehicles. On the way to a fully autonomously driving vehicle, different levels of automated driving have to be mastered as depicted in Tab. 1 and defined, for example, by [1]. With an increasing automation level, the execution, monitoring, and fallback performance are increasingly handled by the system and not by the human driver, increasing the requirements for the sensor system. As shown e.g. in [2] radar sensors are a key technology to enable Level 5 full automation. In contrast to video cameras and laser scanners, a radar sensor is nearly independent of severe weather and light conditions and even remains operational in complete darkness and snowfall. By exploiting the reflections of the electromagnetic waves between road surfaces and the underbody of vehicles it is even possible to detect hidden targets behind other vehicles.

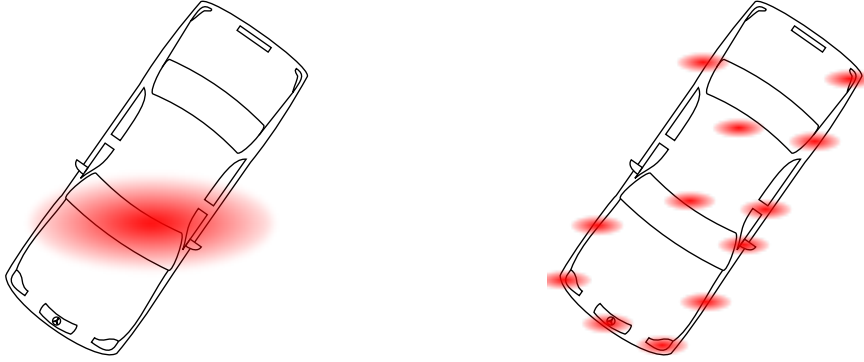
1.1 Some Key Tasks towards Autonomous Driving

High-Resolution Capabilities: Enabling Advanced Driver Assistance Functions

With a radar sensor the radial distance, velocity, and angle of targets can be measured. Key parameters are the accuracy of the measurement and the resolution, i.e. the ability to distinguish close targets. For certain driver assistance functions, typically SAE Level 1 cf. Tab. 1, it was sufficient that a radar sensor can distinguish different objects

SAE Level		Human Tasks		System Tasks
0 No Automation		<ul style="list-style-type: none"> • Execution of steering, velocity control • Environmental perception 		<ul style="list-style-type: none"> • none
1 Driver Assistance		<ul style="list-style-type: none"> • Part of steering/velocity control • Observation of system • Environmental perception 		<ul style="list-style-type: none"> • Part of steering/velocity control
2 Partial Automation		<ul style="list-style-type: none"> • Observation of system • Environmental perception 		<ul style="list-style-type: none"> • Execution of steering/velocity control
3 Conditional Automation		<ul style="list-style-type: none"> • Interaction when requested 		<ul style="list-style-type: none"> • Execution of steering/velocity control • Environment perception
4 High Automation		<ul style="list-style-type: none"> • Human doesn't need to respond in time 		<ul style="list-style-type: none"> • All driving mode-specific tasks handled by system • System goes in error case in a safe state
5 Full Automation		<ul style="list-style-type: none"> • none 		<ul style="list-style-type: none"> • Full-time performance under all roadway and environmental conditions

Tab. 1: Levels of automated driving defined by [1]. The clock symbol indicates which part of the time of travel is handled by the human or by the system each on it's own.



(a) With a low resolution sensor an extended target is detected as a single point target, because only one scattering centre can be distinguished on the object. (b) Only by using high-resolution radar sensors different scattering centres on a target vehicle can be distinguished.

Fig. 1: Comparison of the resulting detection of a target vehicle with a low-resolution sensor in (a) and with a high-resolution sensor in (b). The red blurred ellipses describe the distinguishable scattering centres on the target vehicle.

and estimate one or a low number of scattering centres per object regardless of size [3], cf. Fig. 1 (a). However, a vehicle has many different scattering centres resulting from different curvatures, corners, and slots as mentioned in [4,5] and shown in [6]. They can be measured using a high-resolution sensor as shown in Fig. 1 (b). In this example a higher angular resolution is necessary, which can be achieved with a larger antenna aperture as later explained. Additionally, a high Doppler resolution is helpful to distinguish different radial velocities of the target. As described later on, the modulation parameters have to be adapted for a higher Doppler resolution. Signal processing algorithms can be applied as well to achieve a higher resolution as presented in [7–9].

Current and future automotive radar sensors mainly operate in the 77–81 GHz frequency range as this part of the spectrum is defined by the ITU [10] for future automotive radar sensors. Furthermore, the European Union [11] and the United States [12] have already allocated this frequency band. The European, and therefore also the German [13] regulations, mention a maximum radiated average power spectral density of -3 dBm/MHz inside the vehicle and -9 dBm/MHz outside the vehicle. For the United

States the limitation is given by a maximum equivalent isotropically radiated power (*EIRP*) of 50 dBm within this frequency band. Additionally, the European as well as the American regulation specify a maximum peak power of 55 dBm (*EIRP*). A second frequency band around 24 GHz that is currently being used will not be available worldwide in the future as new vehicles using this frequency range will not be permitted after 2018 for example in Germany [14].

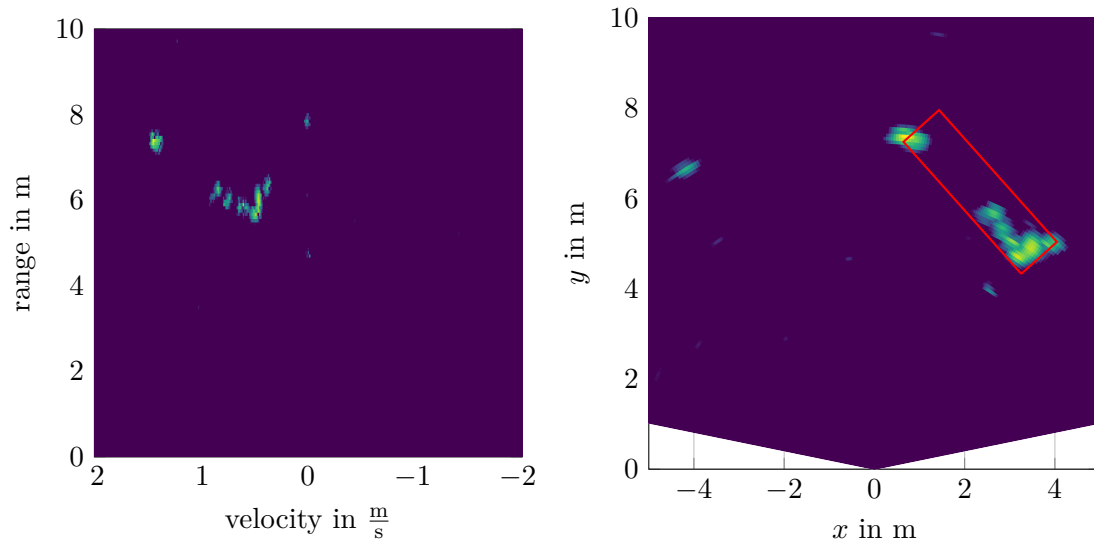
An example of an urban scenario, where a target vehicle is measured with an experimental radar sensor, is depicted in Fig. 2. In the range-Doppler evaluation in (a) the velocity distribution of the moving object can be seen. Applying an angle estimation the contour becomes visible in (b). The video image in (c) is used for validation purposes and shows the measured scene. It can be seen that the moving object is detected with several reflections.

Vehicle Manoeuvre Planning: Dimension, Orientation, and Motion State Estimation of Target Vehicles

The dimension, orientation, and motion state of target vehicles can be used by an autonomous vehicle to plan its driving manoeuvres. High-resolution radar sensors can extract the dimension and orientation of target vehicles [15,16], cf. Fig. 2 (b). Using the orientation it is possible to detect lane changes faster than with a conventional tracking filter, as the filter usually needs several steps to predict the motion correctly. With two radar sensors it is even possible to estimate the complete motion state, for example the orientation and the movement vector including the yaw rate of a target vehicle [17].

Vulnerable Road User Detection and Classification: Micro-Doppler Analysis

For the operation in urban areas, vulnerable road users, such as pedestrians or cyclists, must be detected and classified [18]. As the reflected power from those road users is much lower than from vehicles, the radar sensor must be sensitive for weak targets [19]. Due to the movement of pedestrians various different Doppler velocities can be measured using the micro-Doppler effect [20], cf. Fig. 3. In [21] the authors provide measurement results



(a) The range-Doppler evaluation of the target vehicle. (b) The x - y representation of the target vehicle with estimated orientation (—) as described in [15, 16].



(c) Camera image of the measured scenario.

Fig. 2: Measurement of a target vehicle with an experimental radar sensor. The shown measurements are top view, while the camera image is a side view.

of such vulnerable road users using a high-resolution radar sensor.

Self Localisation: Ego Motion and Position Estimation using Doppler Distribution of Radial Velocities and Gridmaps

For self localisation the precise knowledge of the own motion and position, also called ego motion and position, is important. The motion and position can be determined using radar sensors [22,23] more robustly and with fewer errors during highly dynamic manoeuvres compared to standard vehicle odometry [2]. Additionally, landmarks are often used for self localisation [2,24] by recognising prominent, strongly reflective objects in the environment.

360° Environmental Perception: Multi Radar Sensor Setup

To operate at the full automation level, a multi radar sensor setup is necessary [2], such as the one used in the autonomous vehicle “Bertha” [25] in Fig. 4. With such a setup a 360° environmental perception is possible which is necessary for crossings, roundabouts, and overtaking manoeuvres. The requirements for the radar sensors differ for urban and highway applications. Either the sensors can operate at different modi, such as a long or a short range mode, or different sensors are necessary. Usually, the mode of operation determines the maximum unambiguously covered distance and velocity and the corresponding field of view.

Robustness: Interference Mitigation

With a high market penetration of radar sensors, the possibility of interference rises dramatically. For higher automation levels permanent situation awareness is paramount and sudden blindness, overlooking weak targets, or the detection of ghost targets must be avoided at all times. Hence, a possible harmful interference should be at least detected and in the best case mitigated. Therefore, different interference cases must be evaluated based upon the used modulation formats.

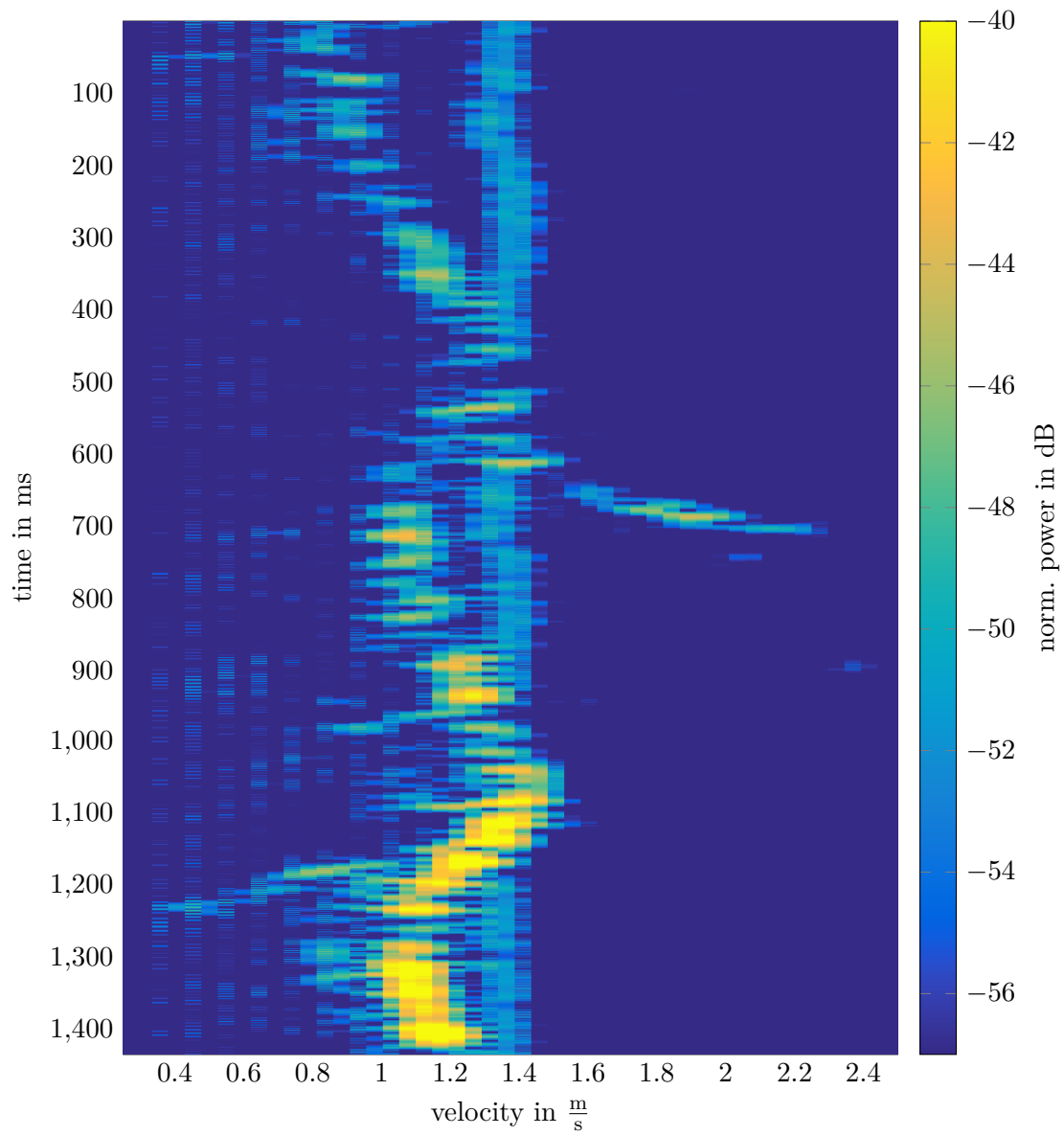


Fig. 3: Velocity distribution of a walking pedestrian over time. The nearly constant velocity component is the main body part, the changing parts correspond to the arms and legs.

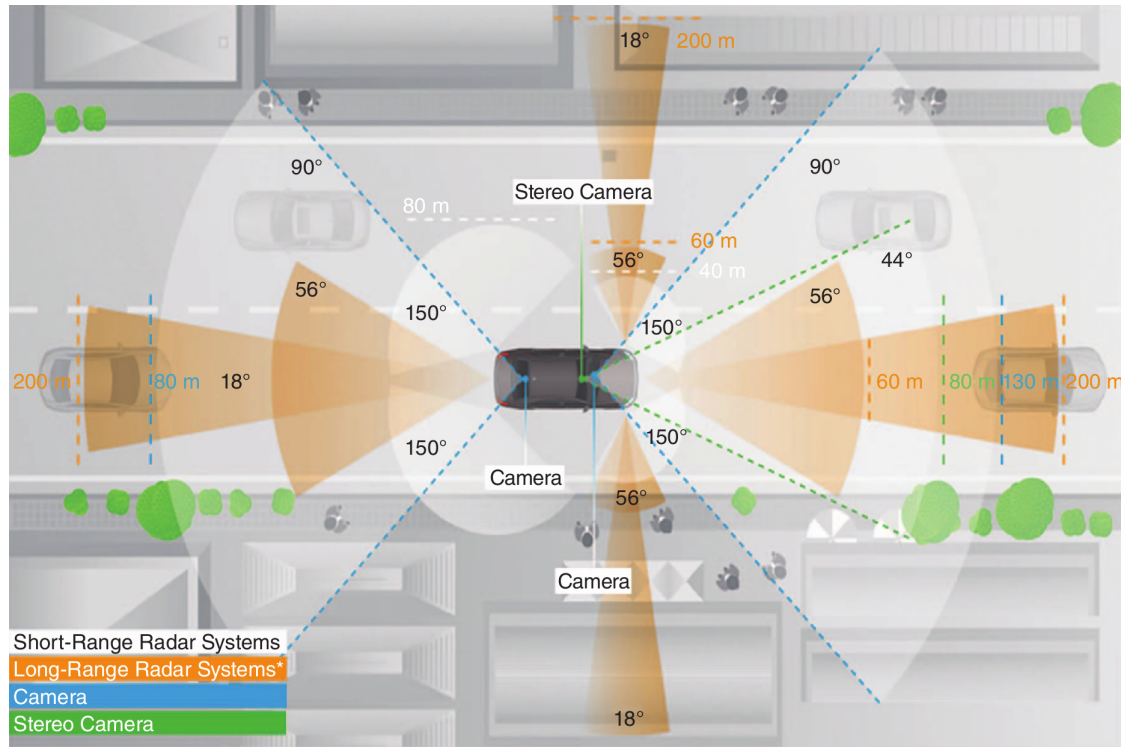
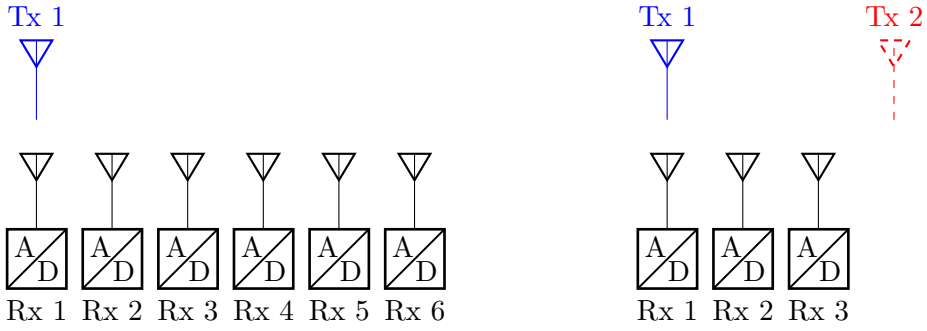


Fig. 4: Sensor setup for the autonomous vehicle “Bertha”. Image taken from [25].

Mass Production: Demand for Low-Cost Hardware

In order to equip nearly every vehicle with one or several radar sensors to achieve 360° coverage, a single sensor must be as inexpensive as possible. Therefore, the hardware requirements should be kept as low as possible, which means simple signal generation, small number of analog-to-digital converters, and sampling frequencies in the lower MHz range.

An example to lower the hardware requirements is presented for direction-of-arrival (*DoA*) estimation. A better *DoA* estimation occurs if the aperture of the receiving antenna elements is large. A large aperture can be achieved with an increased number of receiving elements as in the classic approach shown in Fig. 5 (a). As every receiving element requires an analog-to-digital converter, the hardware effort increases as well as the required memory to store the sampled data. By using a multiple-input multiple-output



(a) The classic *SIMO* case with one transmitter and six receivers. (b) With the *MIMO* realisation using two transmit antennas the number of receivers and therewith the number of analog-to-digital converters can be reduced.

Fig. 5: Comparison of a classic *SIMO* case with the corresponding *MIMO* realisation resulting in the same virtual aperture size.

radar (*MIMO*) setup the aperture can be increased, while maintaining a lower number of required analog-to-digital converters. Usually, the number of transmitting elements is increased while a reasonable amount of receiving elements is chosen as depicted in (b). If three transmitters and eight receiving elements are chosen, the virtual aperture consists of 24 elements. To operate a *MIMO* radar, orthogonal waveforms are necessary. Different algorithms exist to perform the *DoA* estimation based on the different received signals [26], for example in the Bartlett beamformer, subspace methods [27], or maximum likelihood approaches [28]. If the virtual antenna elements are equally spaced, the Bartlett beamformer can be interpreted as a simple Fourier transform. A performance comparison between different *DoA* algorithms as function of the signal-to-noise ratio is given in [29].

To achieve a high spatial resolution, the modulation format is a crucial element, as it dictates all further signal processing. The requirements for the ideal modulation format is high resolution; multiple targets should be detectable and distinguishable, and the hardware demands must be as low as possible to allow mass production. As hardware capabilities continuously improve, an outlook to more powerful modulation

formats is given in the following. Smart signal processing of the modulation formats can additionally decrease the required hardware effort.

This article is organised as follows. In the next section different modulation formats are discussed. Section 3 explains reasons for interference and Section 4 presents possible interference mitigation schemes. Afterwards, in Section 5, a summary and conclusion are given.

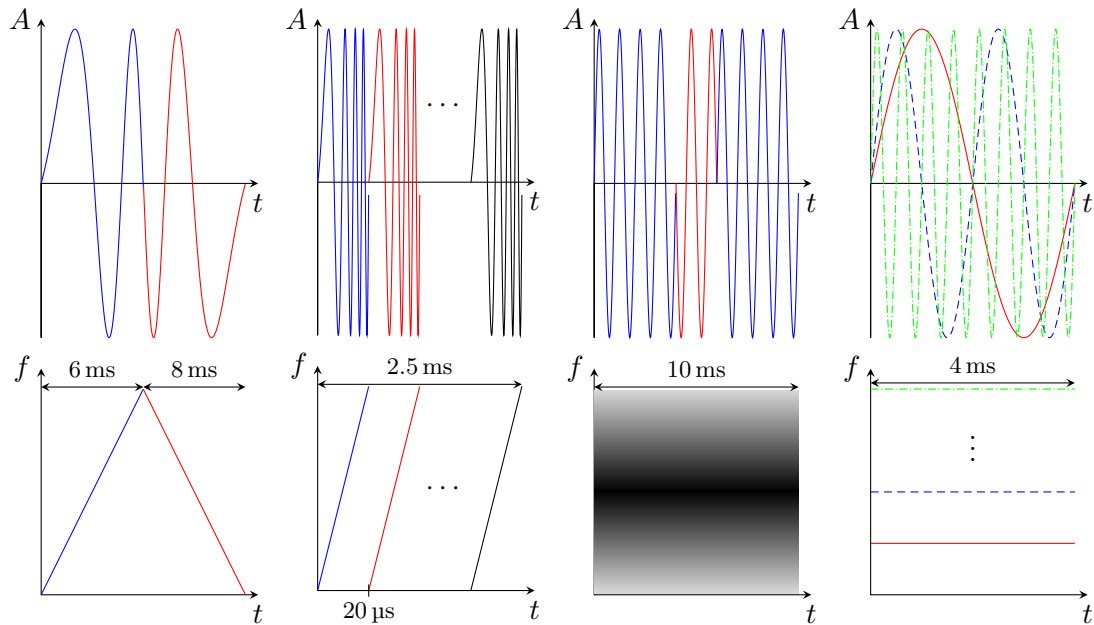
2 Automotive Radar Modulation Schemes

In most radars sensors, e.g. [30], the state-of-the-art *chirp-sequence* modulation format is applied, which is the successor of the well-known frequency modulated continuous wave (*FMCW*) modulation format. With the ongoing development of faster analog-to-digital converters (*ADC*), the application of digital modulation formats such as code modulation or orthogonal frequency division multiplexing (*OFDM*) becomes feasible. Therefore, these modulation formats are discussed in the following.

2.1 Often Used: FMCW with Slow Ramps

The key idea of the classic *FMCW* modulation scheme is to transmit linear frequency ramps with different slopes as depicted in Fig. 6 (a). The transmit time is usually in the range of a couple of milliseconds and the number of transmitted ramps is limited. This realisation is also called *slow ramp* modulation. The transmit signal is reflected by a target and the received signal is mixed with the transmit signal [31,32]. After the down-conversion each reflection from a target results in a sinusoidal signal component after mixing, which depends on the range to the target and the Doppler shift. If the bandwidth of the transmit signal typically is within the range of a GHz, the resulting baseband signal is in the range of several hundred kHz. Hence, the baseband signal can be sampled after an anti-aliasing low-pass filter with a slow low-cost analog-to-digital converter.

The baseband signal, also called the *beat signal*, consists of the range and Doppler velocity of the target. In order to distinguish the two components, different ramp slopes are required. To resolve multiple targets the number of different ramp slopes must be increased accordingly [32].



(a) *FMCW* usually transmits ramps with different slopes. Depicted are an up and a down ramp. (b) *Chirp-Sequence* (*CS*) uses, e.g., 128 frequency chirps of short duration. (c) A constant carrier signal is modulated with a sequence in code modulated radars (*PN*). (d) *OFDM* uses several orthogonal subcarriers which carry the encoded information.

Fig. 6: Overview of different modulation formats in the time domain (top) and frequency domain (bottom). In (a) *FMCW* is depicted with an increasing and decreasing frequency ramp, while in (b) chirp-sequence uses fast chirp signals which are more often repeated. The *PN* modulation in (c) switches the carrier signal fastly with a *BPSK* modulation in this example. The corresponding spectrum shows the applied window function, in this case a Hann window. The *OFDM* signal in (d) uses the whole spectrum with several subcarriers.

Challenging Task in Automotive Environments: Multi Target Scenarios

The typical automotive environment consists of multiple targets, which must be discriminated. With the classic *FMCW* and a reasonable number of different ramp slopes, only a limited number of different targets can be distinguished in a single measurement. Usually, there are more targets present than can be detected unambiguously. This can be either solved by tracking targets over time or with the following *fast ramp* modulation scheme.

2.2 State-of-the-Art: Fast Ramps / Chirp-Sequence Modulation

In the slow ramp procedure the baseband signal depends on the range and the Doppler. If a single frequency ramp is steep, cf. Fig. 6 (b), the range dependent part dominates the baseband signal and the Doppler dependency can be neglected for a single ramp [32,33]. Thus, the Doppler estimation requires a sequence of frequency chirps, which motivates the name of this modulation format as *fast ramps* or chirp-sequence modulation. As the range and Doppler information is separated, a two-dimensional Fourier transform can be used for evaluation.

The advantage compared to the slow ramp procedure is that fast ramp modulation is capable of distinguishing multiple targets in a single measurement. As a drawback of the steeper ramps, the resulting baseband frequencies are typically in the range of several MHz which increases the sampling effort.

Influence of Key Modulation Parameters

Key parameters of the chirp-sequence modulation are depicted in Fig. 7 and listed in Tab. 3. The bandwidth B is directly linked to the range resolution ΔR , while the chirp repetition time T_r influences the unambiguously detectable Doppler frequency v_{\max} . The sampling frequency f_s limits the maximum range. The total measurement time $T=L T_r$ affects the achievable Doppler resolution Δv [34]. The time between two consecutive

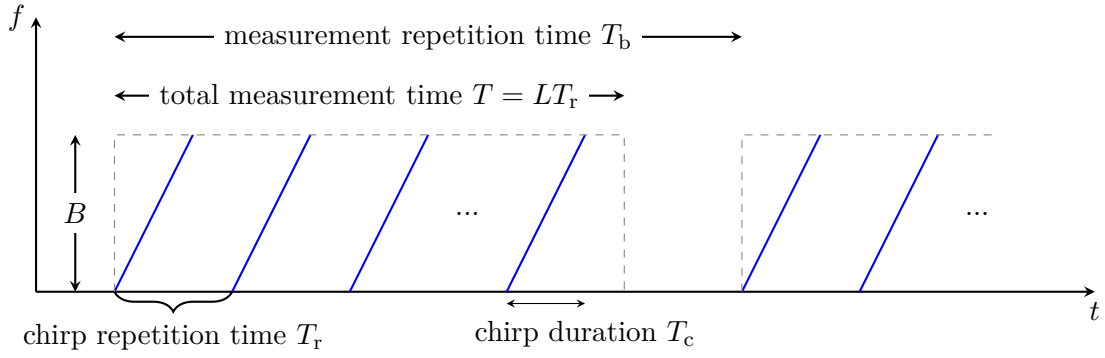


Fig. 7: Key modulation parameters of the state-of-the-art chirp-sequence modulation scheme.

Parameter	Dependency
ΔR	$\approx \frac{c}{2B}$
Δv	$= \frac{c}{2f_c T}$
R_{\max}	$= \frac{cT}{2B} \left(\frac{f_s}{2} - \frac{2f_c v_{\max}}{c} \right)$
v_{\max}	$= \frac{c}{2f_c} \left(\frac{f_s}{2} - \frac{2BR_{\max}}{cT} \right)$
ADC rate	$\leq 1 \text{ MHz (typical)}$

Tab. 2: Parameter dependencies of slow ramp modulation.

measurements T_b is the update rate and is important in a fast changing environment. The similarity to the slow *FMCW* modulation scheme can be seen when comparing the parameter dependencies in Tab. 2.

Enhancing the Unambiguous Doppler Velocity

Aliasing effects due to under-sampling in the range domain can be removed through a low-pass filter before the analog-to-digital conversion. Fast moving targets can cause ambiguities as the Doppler domain cannot be filtered. Therefore, the unambiguous velocity should be as large as required for the respective application. To detect high Doppler velocities either the chirp repetition time must be lowered or the modulation format must be adapted. Faster frequency ramps are more challenging to be generated linearly and increase the sampling effort as the frequency of the resulting beat signal is

Parameter	Dependency
ΔR	$\approx \frac{c}{2B}$
Δv	$= \frac{c}{2f_c L T_r} = \frac{c}{2f_c T}$
R_{\max}	$= \frac{c T_c}{4B} f_s$
v_{\max}	$= \frac{c}{4f_c T_r}$
ADC rate	≤ 10 MHz (typical)

Tab. 3: Parameter dependencies of chirp-sequence modulation.

increased.

One possibility for an adaption of the modulation format is to alter the repetition times in consecutive measurements and apply the Chinese remainder theorem (*CRT*) [33]. Other authors suggest adapting the modulation format using the *interlaced chirp-sequence* approach as presented in [35, 36]. The basic idea is that consecutive frequency ramps have increasing centre frequencies. Sampling points of different frequency ramps can then be evaluated as a resulting long frequency ramp with fast repetition rates to enhance the unambiguous Doppler domain.

Increasing Angular Resolution: Application of MIMO

As mentioned previously, orthogonal waveforms are required to associate different signals with their corresponding transmitters. As presented in [37, 38], for chirp-sequence radars, *time-division*, *frequency-division*, or *code-division* multiplexing is typically used. For *time-division* multiplexing the different transmitters are active one after another. As time passes between the consecutive measurements of the transmit antennas, the angular phase information is corrupted by Doppler shifts from moving targets. This error is usually either neglected for small velocities or is compensated by a double or overlapping element in the virtual aperture [39]. In [40] it is shown that such an overlapping element is not required and that the motion compensation can be resolved with smart signal processing. For *frequency-division* multiplexing the transmit antennas are

active at the same time but at different centre frequencies. Each target is therefore detected at different beat frequencies. *Code-division* multiplexing exploits orthogonal codes. Each transmit signal is encoded by an unique orthogonal code and recovered at the receiver [41].

2.3 A Code Division Modulated Approach: Phase-Modulated Continuous Wave Radar

Code-modulated radars (spread spectrum, pseudo-noise (*PN*), phase modulated continuous wave (*PMCW*)) transmit a wide-band code sequence that is modulated on a high-frequency continuous wave (*CW*) carrier signal, cf. the schematic in Fig. 6 (c). On the receiver side, the signals are down-converted and correlated with the transmitted code sequence as depicted in Fig. 8. The codes have a short duration T_{s2s} such that the Doppler effect does not influence the correlation. Peaks in the correlation yield the time of flight and thus the object distance. A *PN* radar transmits a series of code sequences for Doppler extraction, as the phase of the continuous-wave carrier changes between the transmitted sequences. A Fourier transform across all transmitted sequences yields the velocity information; however, in contrast to chirp-sequence, *PN* radars require an I-Q receiver in order to distinguish positive and negative velocities. A proper selection of the code offers low range side lobes or a low cross-correlation with other codes [42]. The parameter dependencies are summarized in Tab. 4 and are very similar to the parameter dependencies of chirp-sequence radars.

An important aspect of *PN* radars is the realization of the correlation of the receive signal. A correlation is possible in the digital domain after sampling the receive signal [44]; however, this requires a very high sampling rate, as the baseband bandwidth is equal to the RF modulation bandwidth. Consequently, high data rates have to be handled. Such systems for the 79 GHz band with bandwidths up to 2 GHz and a focus on automotive applications have been discussed in [45–47]. The high sampling rate

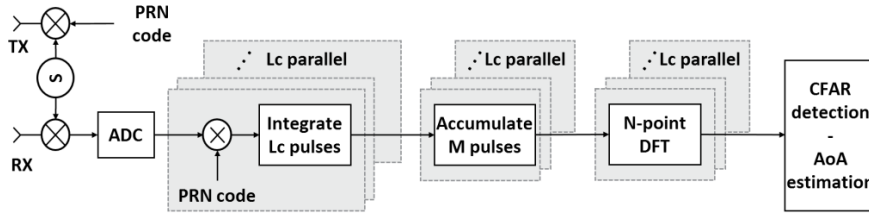


Fig. 8: Schematic of a code-modulated radar with a fully-digital processing. Fig. taken from [43].

Parameter	Dependency
ΔR	$\approx \frac{c}{2B}$
Δv	$= \frac{c}{2f_c L T_s 2s} = \frac{c}{2f_c T}$
R_{\max}	$= \frac{c T_s 2s}{2}$
v_{\max}	$= \frac{c}{4f_c T_s 2s}$
ADC rate	$\leq 1 \text{ GHz}$ (typical, I and Q channel)

Tab. 4: Parameter dependencies of code modulated radars.

leads to a large integration gain. The authors of [48] use this fact to reduce the ADC resolution to only 4 bits what reduces the data rate significantly. They show that their sensor is still able to detect pedestrians at a distance of 30 m. The correlation can also be done in the analog domain with time-delayed versions of the code sequence for all range cells one after another [49–52]. This offers reduced effort in signal processing, but leads to a high measurement time when many different range cells are measured. Many parallel correlators can compensate this increase in measurement time, but lead to more hardware effort.

The application of orthogonal codes for multiple transmitters allows multiple sensors to operate at the same time in the same frequency band without undesired interactions. Such a time- and frequency-parallel *MIMO* system without the need for multiplexing is presented in [43] and in [53].

2.4 A Digital Modulation Format: Orthogonal Frequency Division Multiplexing

Due to the progress in digital technology in the past few years, approaches that shift the major effort of radar systems to the digital domain have become more favorable. Such a system can be seen as a software defined radio (*SDR*) that provides capabilities that are hard to match with common single-carrier radars. This includes unmatched flexibility, adaptivity, robustness, calibration opportunities, and efficient channel usage.

A multi-carrier modulation scheme suitable for an *SDR* and radar detection is orthogonal frequency division multiplexing (*OFDM*) which is also widely used in communication technology [54].

OFDM dates back to the 1960's [55, 56] but did not attract attention for radar applications until the last decade. The idea of a multi-carrier radar scheme was first brought up by Levanon [57] in 2000. Driven by the idea to combine radar and communications [58–60], various signal processing improvements [61–63] have been presented since then.

An *OFDM* signal consists of coded signals transmitted on multiple carrier frequencies, called subcarriers, continuously and in parallel, as depicted in Fig. 6 (d). All transmit symbols of all subcarriers are modulated with the same distinct code, for instance *QPSK*, and have a constant symbol length of T_{sym} . To maintain orthogonality, the N subcarriers are uniformly spaced with $\Delta f = 1/T_{\text{sym}}$. This results in a total bandwidth of $B = N\Delta f$. Fig. 9 shows the spectrum of an *OFDM* signal with three subcarriers, where the spectrum of each individual subcarrier results in a sinc-function due to its finite length. Since the carrier spacing is reciprocal to the symbol length, the maximum of every single sinc-function is located where all other functions are zero. Therefore, the signals are orthogonal without any inter-carrier interferences (*ICI*).

The baseband signal generation of the *OFDM* signal can be easily realized in the digital domain. The modulation on the individual subcarriers is achieved by applying

Parameter	Dependency
ΔR	$\approx \frac{c}{2B}$
Δv	$= \frac{c}{2f_c T_{\text{sym}} M}$
R_{max}	$= \frac{c T_{\text{cp}}}{2}$ (no ISI)
v_{max}	$= \pm \frac{c}{32 f_c T}$ (typical, no ICI)
ADC rate	≤ 1 GHz (typical, I and Q channel)

Tab. 5: Parameter dependencies of *OFDM*.

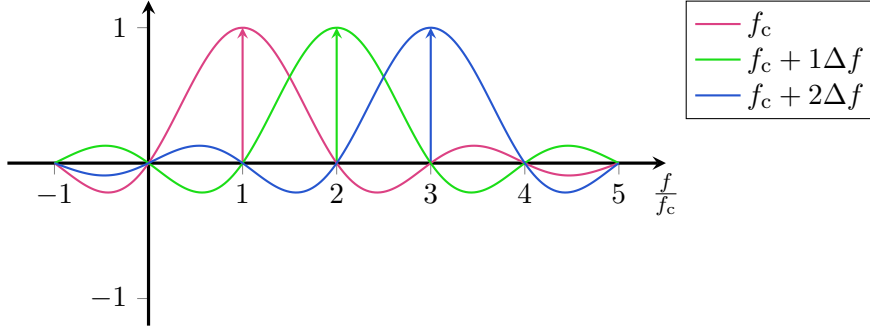


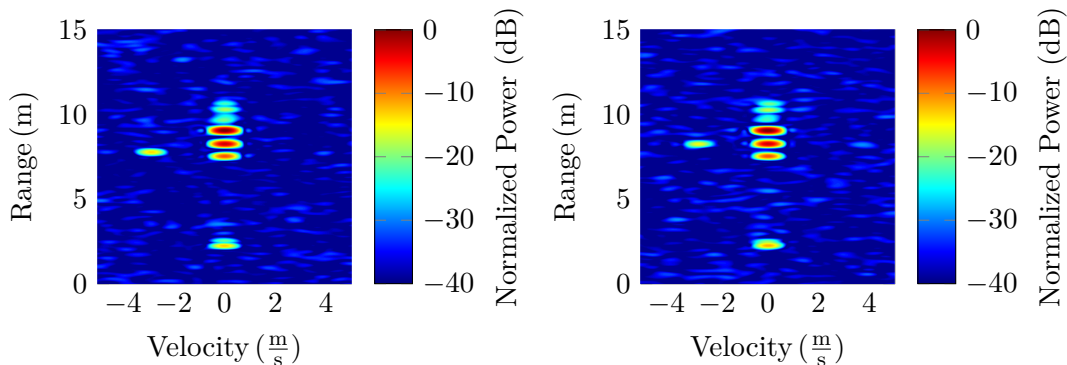
Fig. 9: Spectrum of an *OFDM*-signal with three subcarriers.

an *IFFT* to all complex symbols $d_{n,m}$ of all $n=0, \dots, N-1$ subcarriers for each time instance $m=0, \dots, M-1$. A sequence of M *OFDM* symbols is called a frame. To prevent intersymbol interference (*ISI*) due to delayed receive signals and multipath effects, each *OFDM* symbol is extended by a so-called cyclic prefix (*CP*). The *CP* is a cyclic repetition of each signal that is added at the beginning of each symbol using a copy of length T_{cp} of the symbol tail. The digital baseband signal is *DA* converted, modulated to the carrier frequency, and transmitted through the antenna. After reception, the signal is down-converted to baseband and then digitized. Next, the *CP* is removed and the modulation on the sub-carriers is reversed using an *FFT*. In communications, the receive symbols are identified and evaluated in the next step. For radar applications, the channel information $D(n, m)$ is obtained by removing the known baseband transmit symbols from the baseband receive signal. Applying an *IFFT* along the different subcarriers n and an *FFT* along subsequent symbols m , joint range, and Doppler information of all targets

are extracted from D , yielding an actual two-dimensional range-velocity profile, quite similar to the chirp-sequence evaluation. As in the chirp-sequence, the range resolution is directly proportional to the channel bandwidth B , which is equal to the baseband bandwidth in *OFDM*. The Doppler resolution depends on the total observation time. The maximum unambiguous range depends on the symbol time and the unambiguous Doppler on the carrier spacing, which is also directly linked to the symbol time.

The large baseband bandwidth has the drawback that a large bandwidth has to be filtered and sampled at the receiver. Since such hardware is expensive and hard to realize, only a fraction of the required bandwidth is achievable with reasonable effort, making it unusable for automotive applications as the range resolution would not meet the requirements. A solution is to use a smaller bandwidth that is realizable with low-cost hardware and to regain the full resolution of the large RF bandwidth by using different carrier frequencies in a single frame and applying suitable signal post-processing [64–66]. The different discrete carrier frequencies can be realized in a stepped fashion to cover the full channel bandwidth per measurement cycle. Through such a carrier scheme, a full resolution radar image can be obtained at the receiver having the same range and Doppler resolution as the conventional *OFDM* signal with large bandwidth, as can be seen in Fig. 10.

Another advantage of *OFDM* becomes apparent in a *MIMO-OFDM* radar: multiple transmitters can be used simultaneously as long as no subcarrier is used by two transmitters at once. To distribute the subcarriers to the transmitters, spectral interleaving is applied [67, 68]. In the case of P transmit antennas, every P -th subcarrier is assigned to one antenna. This guarantees that the individual transmit signals do not interfere but use the same bandwidth that is approximately equal to the baseband bandwidth of an equivalent *OFDM* signal without interleaving. Maintaining the bandwidth does not result in a reduction of the range resolution; however, sharing the carriers reduces the maximum unambiguous range by the number of transmitter.



(a) High-resolution reference with 1.024 GHz. (b) Eight frequency steps with 128 MHz each.

Fig. 10: 77 GHz *OFDM* radar measurements with 1 GHz RF bandwidth. In (a) the full baseband bandwidth of 1 GHz and in (b) only 128 MHz baseband bandwidth is used. The same RF bandwidth and range resolution is reached using proper signal processing. Fig. taken from [64].

3 Interference between Automotive Radars for Different Modulation Schemes

There are high requirements on modulation bandwidth, observation time, and fast update rates for automated driving applications. Additionally, an environment perception of 360° in azimuth and the application of height estimation are desired. This requires multiple radar sensors per car transmitting to and receiving from surrounding vehicles. If many cars are equipped with a multitude of radar sensors for driver assistance systems, there is a high probability that the sensors interfere with each other or even with stationary radars, integrated into the infrastructure used for traffic monitoring. Such interferences are an important issue with respect to the sensor robustness, as they can reduce the detection capability or lead to false targets. The problem is especially critical in dense traffic situations. To underline the significance of the problem, the receive power of an object in distance R given by the radar equation,

$$P_R = \frac{P_T G_T G_R \lambda^2 \sigma}{(4\pi)^3 R^4} \quad (1)$$

is compared with the Friis equation for an interference source in the same distance,

$$P_{\text{int}} = \frac{P_T G_T G_R \lambda^2}{(4\pi)^2 R^2}. \quad (2)$$

It is assumed that the transmit power P_T , the antenna gain G_T , and the wavelength λ of the interfered and the interfering sensor are in the same order of magnitude. The receive antenna gain G_R is in both equations related to the interfered sensor. When comparing the equations it can be noticed that the receive power of targets decreases with R^4 , while the interference power decreases only proportional to R^2 . Thus, the problem is even more critical for distant objects. Based on the above equations, [69] shows that the power level of a target with a radar cross section (RCS) of 1 m^2 in 200 m distance is about 56 dB below the interference power received from the same distance.

Because of the interference problem, sensors need sufficient countermeasures for reliable functionality in interference situations. The effects and the probability of interference strongly depend on the modulation format. The occurrence of interference between two *FMCW* radars depends on multiple factors: the transmit frequencies, the transmission times, the ramp slopes determining the duration, and how frequent the interference occurs. While short spikes affecting a few samples in the time signal will be the most common effect in such a setup, leading to wide-band noise increase in the spectrum [69–71], the probability for frequent and long-acting interferences is small — for identical modulation parameters it is below 10^{-3} [70] for a single measurement.

When interference between chirp-sequence-, *PN*-, or *OFDM*-modulated radars are considered, the problem is much more critical. The latter modulation formats have a larger occupancy of the available spectrum during a measurement cycle and have higher receiver bandwidths, especially the *OFDM* and *PN* modulations. When even more sensors operate at the same time in the $76\text{--}77 \text{ GHz}$ or $77\text{--}81 \text{ GHz}$ frequency band, it is unavoidable that interferences occur. Interference generation between automotive

radars and the most common interference effects are discussed for the previously described modulation formats in the next sections, followed by an overview of potential countermeasures in the field of automotive radars.

3.1 FMCW and Chirp-Sequence Interference

Interference between an *FMCW* and a chirp-sequence radar is depicted in Fig. 11. The *FMCW* ramp regularly intersects the fast frequency chirps, and each time mutual interference occurs. Various investigations [69, 72] showed that this kind of interference adds time-limited wide-band distortion in the baseband as shown in the middle part of Fig. 11. The time-limitation originates from the anti-aliasing low-pass in the receiver; its bandwidth is indicated in the upper part of the figure. Because of the large ramp slopes and the resulting high baseband frequencies, the filter bandwidth is much wider for chirp-sequence than it is for *FMCW* modulated radars.

The bottom part of Fig. 11 compares the interfered and interference-free spectrum of the depicted signal. The increased noise level is especially critical for the reliable detection of targets with a low radar cross section (*RCS*), like bicycles or pedestrians. Experiments in [73] show an increased noise level of up to 20 dB in an *FMCW* radar suffering of interference from a *CW* radar in 10 m distance.

3.2 OFDM and PN Interference

The high occupancy of modulation bandwidth over time and the wide receiver bandwidth in the range of several MHz in chirp-sequence radars lead to an increased interference risk compared to slow-ramp *FMCW* radars. This effect is even more relevant for wide-band *OFDM* and PN modulation schemes. The receiver bandwidth covers all *OFDM* carriers during the whole measurement duration. Instead of the time-limited interferences in Fig. 11, ubiquitous disturbance is present.

Interference between linear frequency modulated and wide-band *OFDM* modulated

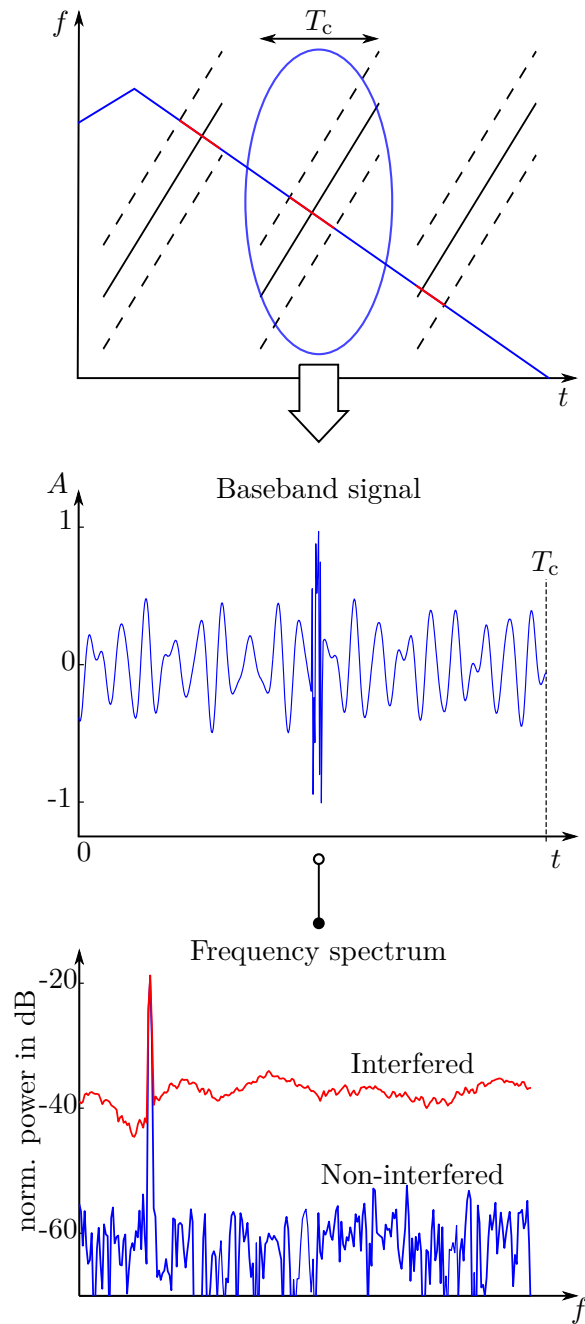


Fig. 11: An *FMCW* and a chirp-sequence modulated radar operate in the same frequency band. Interference (—) occurs in the chirp radar as long as the *FMCW* signal falls into the receiver bandwidth (---). In the baseband frequency spectrum the noise floor is raised compared to an interference-free frequency ramp.

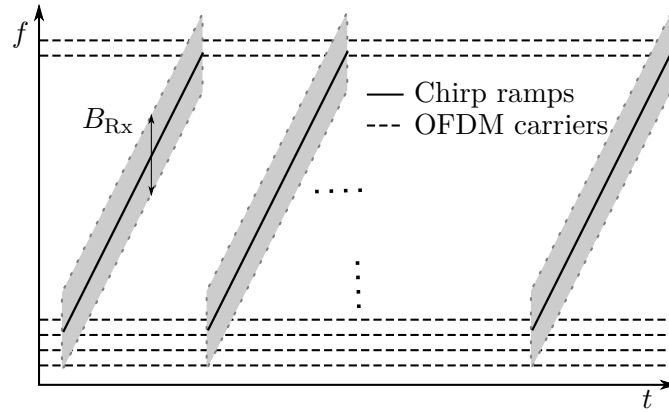


Fig. 12: Interference between an *OFDM*- and a chirp-sequence-modulated radar.

radars also leads to an increased overall noise level in both system types [74, 75]. While an *OFDM* signal is affected by the full *FMCW* or chirp-sequence signal power, a linear frequency modulated radar is only disturbed by that part of the *OFDM* signal that falls into the receiver bandwidth, cf. Fig. 12. The interference power in the *FMCW* or chirp-sequence receiver is proportional to the area indicated by the gray parallelogram in Fig. 12 [75].

In *PN* radars similar interference effects are expected as in *OFDM* modulated ones. The large receiver bandwidth leads to the reception of a lot of interference power during the whole measurement time. As long as the interference is uncorrelated to the code sequence, it will result in a wideband noise increase.

4 How can we Handle the Interference Threat?

The above described interference can severely degrade the performance of radar sensors. In order to mitigate interference effects, the interference can be detected and afterwards, countermeasures can be applied.

4.1 Interference Detection

For interference between *FMCW* or chirp-sequence radars several detection algorithms have been developed for the time domain signals. This is done based on the high power and the short duration of the interference in [76]. Other approaches apply matched signal transforms [77] or image processing methods [78] to detect interference. It was shown that *OFDM* interference is very difficult to distinguish from thermal noise in the spectrum of *FMCW* receivers, making a detection more problematic [79]. For *OFDM* radars a detection algorithm similar to the above-mentioned power detectors in combination with an ordered statistic approach is demonstrated in [80].

4.2 Time-Domain Approaches

After the detection of the interfered samples in the time domain data of chirp-sequence signals, those samples can be set to zero to prevent an increase of the noise level in the frequency spectrum [69]. However, zeroing requires a robust detection and raises additional frequency components; these artifacts can be reduced by introducing a window function at the time domain discontinuities [78] or a prediction of the missing data with autoregressive models [81]. It is also possible to estimate and afterwards cancel the interference component [82] from the time signals. This does not suppress the interference completely, but it does not introduce artifacts in the spectrum. These time-domain approaches are well-suited for time-limited interference between linear frequency modulated radars; however, they are not yet tested for interference from and between Code- and *OFDM*-modulated radars. Code and *OFDM* modulations occupy a wide bandwidth during the whole duration of a measurement and therefore cause and suffer from long interference durations. Nevertheless, it is shown in [80] that the interfered data can be removed and subsequently reconstructed through compressed sensing algorithms when interference between multiple *OFDM* radars occurs.

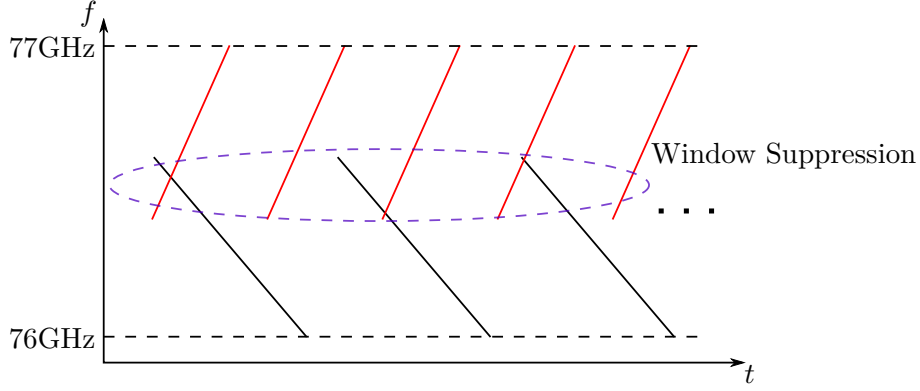


Fig. 13: When frequency regulations limit the capabilities of frequency hopping, the window function still offers good interference suppression – at least for *OFDM* and *CS* radars.

4.3 Frequency Diversity

As long as the frequency band is not yet completely occupied, frequency hopping can be used for interference mitigation independent of the modulation scheme. However, it cannot recover data of measurements which are already corrupted by interference. A simple implementation of frequency hopping is to vary the carrier frequency after each transmission with a pseudo-random selection scheme. It was shown with *FMCW* radars [83] that this already leads to a very low probability of permanent interference between two sensors. However, there is a high probability that interference occurs in several measurements. Another approach suited for chirp-sequence radars is an estimation of an interfering radar's transmit frequency based on the detected interference in the time domain signals [84]. The high number of chirps in each single measurement leads to a robust estimation followed by an adaptive frequency hopping to avoid interference in subsequent measurements. This is suited even more for Code- and *OFDM*-modulations: their wide receiver bandwidth “scans” the modulation bandwidth during the full measurement duration.

If interfering sensors occupy too much bandwidth, interference-free operation might not be possible in a given frequency band. Even in this scenario an adaptive frequency

hopping can align the sensors' bandwidths with the smallest possible overlap, cf. Fig. 13. In this case the window function applied in signal processing of linear frequency modulated radars leads to a good interference suppression, cf. [72]. The same way of windowing is also valid for *OFDM* radars.

4.4 Spatial Masking of Interference Sources

In radar systems with multiple receive channels it is possible to apply a receiver-sided digital beamforming (*DBF*) to suppress signals from an interferer's direction. This direction can be estimated based on the interfered samples of the time signals [77, 85]. With this knowledge the interference is removed from the field of view as depicted in Fig. 14, and desired directions of arrival can be amplified. The opportunities of *DBF* increase with an increasing aperture size and number of receive channels. Although *MIMO* radars offer a large virtual aperture size, this virtual aperture cannot be used for interference suppression. The interference affects only the physical receive array and not the whole virtual aperture. Therefore, interference can only be canceled within the physical receive aperture [86].

Interference suppression by *DBF* is very promising because it is independent of the modulation format of the interfered and the interfering sensor. It is also not required to detect all interfered samples in the time signals, as long as the direction of the interfering signals can be determined. However, desired signals in the direction of the interference cannot be detected anymore. Experimental results for a chirp-sequence system with only four receive channels already show an interference suppression of up to 15 dB [85].

There is one special issue concerning *DBF* in linear frequency modulated radars. As these systems typically do not have an I-Q receiver, the interference energy is spread over multiple directions of arrival because of the image frequency of the interfering signal [86]. In this case a beamformer must take into account multiple directions when forming its beams.

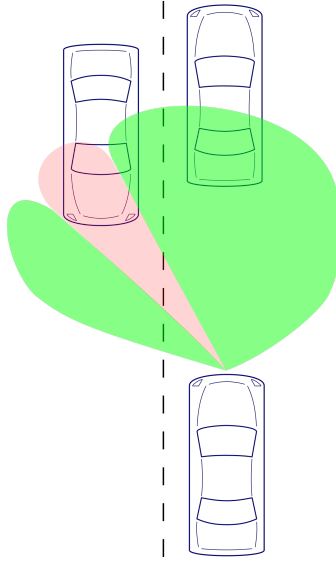


Fig. 14: The beamformer removes the interfering sensor from the field of view.

5 Summary

The key tasks which enable autonomous driving explained in the introduction are used to compare the different presented modulation schemes.

5.1 High-Resolution Capabilities

To enable the detection and classification of vulnerable road users in automotive environments high-resolution and separability of close targets is a key requirement. The lack of real multi-target capability of the slow *FMCW* modulation format is a disadvantage. The enhancement of the *FMCW* scheme, the so-called chirp-sequence modulation, has higher but manageable hardware demands and is therefore the current state-of-the-art approach. To enhance the angular resolution *MIMO* schemes are used which could be realised easier with the digital modulation formats.

5.2 Demand for Low-cost Hardware and Efficient Usage of Resources

Considering the signal generation and sampling of the resulting baseband signal, slow *FMCW* has the lowest hardware demands. Transmitting faster frequency chirps and sampling the higher baseband signals is possible at low cost. Hence, the chirp-sequence modulation format is the current state-of-the-art modulation format and has manageable hardware demands.

Both digital modulation formats, *PN* and *OFDM*, require in the basic scheme a digital-to-analog converter for the signal generation as well as an analog-to-digital converter with the full modulation bandwidth. The advantage of mixing the transmit with the receive signal to gain a low frequent baseband signal is not possible as in *FMCW* or *CS*. As this bandwidth is mostly in the range of a couple of GHz such converters are either not available or the hardware costs are too high for automotive applications. Solutions might be stepped *OFDM* modulations.

5.3 Robustness against Interference

The sensor requirements for automated and autonomous driving make interference an important topic. For *FMCW* and chirp-sequence modulation, interference will not occur during the whole measurement duration, as the baseband bandwidth is much smaller compared to the transmitted bandwidth. This clearly reduces the chance to collect interference power from other sensors compared to both digital modulation formats where the full transmit bandwidth is sampled during the whole measurement duration. It also reduces the chance to transmit interfering power into other sensors.

There exists a multitude of ways to counteract interference effects. Time domain approaches span from the calculation power intensive interpolation of corrupted data to the simple zeroing of interfered samples. They are most effective for short-duration interference, require reliable detection algorithms, and their specific realization depends on the modulation format. Frequency hopping is very cost-effective in terms of implementation

and calculation effort and can offer good performance for interference mitigation. It is, however, limited by the available bandwidth, especially in dense traffic situations when many sensors operate simultaneously. Digital beamforming is effective for all modulation schemes, and it does not require a detection of all interfered samples. While suppressing interferences *DBF* can also amplify directions of interest. On the other hand, the sensor will always be blind towards the direction of the interferer. Furthermore, the performance is limited by the available aperture.

It is not yet clear, what kind of interference countermeasures or mitigation approaches are suited best for the different modulation schemes. It seems reasonable that time domain approaches are helpful in case of short interference durations, for example between linear frequency modulated sensors. However, time domain approaches will suffer in case of long interference durations caused by *PN*- or *OFDM*-modulated radars. Currently, there are not many automotive interference evaluations available for *PN*- and *OFDM*-modulated radars. Further investigations are required to examine which additional effects might have to be taken into account and which approach handles interference best.

6 Conclusion

Enabling autonomous driving has a huge influence on the requirements of radar sensors. Different common modulation formats are introduced and compared regarding the new requirements. To establish a 360° coverage of the environment, a single radar sensor is not sufficient. Together with an increasing number of vehicles equipped with multiple sensors the probability of interference increases. The overview of interference mitigation schemes shows that there are many approaches towards reliable radar operation in multi-sensor scenarios. Once a large number of sensors are operating at the same time, one single approach will not be sufficient. In order to guarantee reliable operation for all scenarios multiple interference countermeasures must be combined.

References

- [1] SAE International, "Taxonomy and Definitions for Terms Related to Driving Automation Systems for On-Road Motor Vehicles," 2016. [Online]. Available: http://standards.sae.org/j3016_201609/
- [2] J. Dickmann *et al.*, "Automotive Radar the Key Technology for Autonomous Driving: From Detection and Ranging to Environmental Understanding," in *IEEE Radar Conference (RadarConf)*, May 2016, pp. 1–6.
- [3] J. Dickmann *et al.*, "Radar contribution to highly automated driving," in *European Radar Conference*, Oct. 2014, pp. 412–415.
- [4] H. Buddendick and T. F. Eibert, "Incoherent Scattering-Center Representations and Parameterizations for Automobiles," *IEEE Antennas and Propagation Magazine*, vol. 54, no. 1, pp. 140–148, Feb. 2012.
- [5] M. Bühren and B. Yang, "Automotive Radar Target List Simulation based on Reflection Center Representation of Objects," in *Workshop on Intelligent Transportation (WIT)*, Hamburg, Germany, Mar. 2006, pp. 161–166.
- [6] M. Andres, P. Feil, and W. Menzel, "3D-Scattering Center Detection of Automotive Targets Using 77 GHz UWB Radar Sensors," in *European Conference on Antennas and Propagation (EUCAP)*, Mar. 2012, pp. 3690–3693.
- [7] M. Andres, W. Menzel, H.-L. Bloecher, and J. Dickmann, "Detection of Slow Moving Targets using Automotive Radar Sensors," in *German Microwave Conference (GeMiC)*, Mar. 2012, pp. 1–4.
- [8] C. Fischer *et al.*, "Adaptive Super-Resolution with a Synthetic Aperture Antenna," in *Proceedings of the 9th European Radar Conference (EuRAD)*, Oct. 2012, pp. 250–253.
- [9] S. Olbrich and C. Waldschmidt, "New pre-estimation Algorithm for FMCW Radar Systems using the Matrix Pencil Method," in *European Radar Conference (EuRAD)*, Sep. 2015, pp. 177–180.
- [10] ITU, "Final Acts WRC-15 – World Radiocommunication Conference," 2015.
- [11] ETSI, "Short Range Devices; Transport and Traffic Telematics (TTT); Short Range Radar equipment operating in the 77 GHz to 81 GHz band; Harmonised Standard covering the essential requirements of article 3.2 of Directive 2014/53/EU," 2017.
- [12] Federal Communications Commission, "FCC-CIRC1707-07," 2017.
- [13] Bundesnetzagentur, "Allgemeinzuteilung von Frequenzen für Kraftfahrzeug - Kurzstreckenradare im Frequenzbereich 77–81 GHz," 2014.

- [14] Bundesnetzagentur, “Allgemeinzuteilung von Frequenzen für Kraftfahrzeug-Kurzstreckenradare im Frequenzbereich 21,65–26,65 GHz,” 2012.
- [15] F. Roos *et al.*, “Estimation of the Orientation of Vehicles in High-Resolution Radar Images,” in *IEEE MTT-S International Conference on Microwaves for Intelligent Mobility (ICMIM)*, Apr. 2015, pp. 1–4.
- [16] F. Roos, D. Kellner, J. Dickmann, and C. Waldschmidt, “Reliable Orientation Estimation of Vehicles in High-Resolution Radar Images,” *IEEE Transactions on Microwave Theory and Techniques*, vol. 64, no. 9, pp. 2986–2993, Sep. 2016.
- [17] D. Kellner *et al.*, “Tracking of Extended Objects with High-Resolution Doppler Radar,” *IEEE Transactions on Intelligent Transportation Systems*, vol. 17, no. 5, pp. 1341–1353, Dec. 2016.
- [18] J. Dickmann *et al.*, “Making Bertha See Even More: Radar Contribution,” *IEEE Access*, vol. 3, pp. 1233–1247, 2015.
- [19] D. Belgiovane and C.-C. Chen, “Bicycles and Human Riders Backscattering at 77 GHz for Automotive Radar,” in *European Conference on Antennas and Propagation (EuCAP)*, Apr. 2016, pp. 1–5.
- [20] V. C. Chen, F. Li, S.-S. Ho, and H. Wechsler, “Micro-Doppler Effect in Radar: Phenomenon, Model, and Simulation Study,” *IEEE Transactions on Aerospace and Electronic Systems*, vol. 42, no. 1, pp. 2–21, Jan. 2006.
- [21] E. Schubert, F. Meinel, M. Kunert, and W. Menzel, “High Resolution Automotive Radar Measurements of Vulnerable Road Users – Pedestrians & Cyclists,” in *IEEE MTT-S International Conference on Microwaves for Intelligent Mobility (ICMIM)*, Apr. 2015, pp. 1–4.
- [22] D. Kellner *et al.*, “Instantaneous Ego-Motion Estimation using Doppler Radar,” in *International IEEE Conference on Intelligent Transportation Systems (ITSC)*, Oct. 2013, pp. 869–874.
- [23] D. Kellner *et al.*, “Instantaneous Ego-Motion Estimation using Multiple Doppler Radars,” in *IEEE International Conference on Robotics and Automation (ICRA)*, May 2014, pp. 1592–1597.
- [24] K. Werber, J. Klappstein, J. Dickmann, and C. Waldschmidt, “Interesting Areas in Radar Gridmaps for Vehicle Self-Localization,” in *IEEE MTT-S International Conference on Microwaves for Intelligent Mobility (ICMIM)*, May 2016, pp. 1–4.
- [25] J. Ziegler *et al.*, “Making Bertha Drive - An Autonomous Journey on a Historic Route,” *IEEE Intelligent Transportation Systems Magazine*, vol. 6, no. 2, pp. 8–20, Summer 2014.

- [26] P. Häcker and B. Yang, “Single snapshot DOA estimation,” *Advances in Radio Science*, vol. 8, pp. 251–256, 2010. [Online]. Available: <http://www.adv-radio-sci.net/8/251/2010/>
- [27] R. O. Schmidt, “Multiple Emitter Location and Signal Parameter Estimation,” *IEEE Transactions on Antennas and Propagation*, vol. 34, no. 3, pp. 276–280, Mar. 1986.
- [28] P. Stoica and K. C. Sharman, “Maximum Likelihood Methods for Direction-of-Arrival Estimation,” *IEEE Transactions on Acoustics, Speech, and Signal Processing*, vol. 38, no. 7, pp. 1132–1143, Jul. 1990.
- [29] M. Schoor and B. Yang, “High-Resolution Angle Estimation for an Automotive FMCW Radar Sensor,” in *International Radar Symposium (IRS)*, 2007.
- [30] Robert Bosch GmbH, *LRR3: 3rd generation Long-Range Radar Sensor*, 2009. [Online]. Available: http://products.bosch-mobility-solutions.com/media/db_application/downloads/pdf/safety_1/en_4/lrr3_datenblatt_de_2009.pdf
- [31] A. Stove, “Linear FMCW radar techniques,” *IEE Proceedings-F on Radar and Signal Processing*, vol. 139, no. 5, pp. 343–350, Oct. 1992.
- [32] V. Winkler, “Range Doppler Detection for automotive FMCW Radars,” in *Proceedings of the 4th European Radar Conference (EuRAD)*, Oct. 2007, pp. 166–169.
- [33] C. Schroeder and H. Rohling, “X-Band FMCW Radar System with Variable Chirp Duration,” in *IEEE Radar Conference*, May 2010, pp. 1255–1259.
- [34] F. Roos *et al.*, “Enhancement of Doppler Resolution for Chirp-Sequence Modulated Radars,” in *European Radar Conference (EuRAD)*, Oct. 2016, pp. 237–240.
- [35] K. Thurn *et al.*, “A Novel Interlaced Chirp Sequence Radar Concept with Range-Doppler Processing for Automotive Applications,” in *IEEE MTT-S International Microwave Symposium (IMS)*, May 2015, pp. 1–4.
- [36] K. Thurn *et al.*, “Concept and Implementation of a PLL-Controlled Interlaced Chirp Sequence Radar for Optimized Range-Doppler Measurements,” *IEEE Transactions on Microwave Theory and Techniques*, vol. 64, no. 10, pp. 3280–3289, Oct. 2016.
- [37] J. J. M. de Wit, W. L. van Rossum, and A. J. de Jong, “Orthogonal Waveforms for FMCW MIMO Radar,” in *IEEE RadarCon (RADAR)*, May 2011, pp. 686–691.
- [38] H. Sun, F. Brigui, and M. Lesturgie, “Analysis and Comparison of MIMO Radar Waveforms,” in *International Radar Conference*, Oct. 2014, pp. 1–6.
- [39] C. M. Schmid, R. Feger, C. Pfeffer, and A. Stelzer, “Motion Compensation and Efficient Array Design for TDMA FMCW MIMO Radar Systems,” in *6th European Conference on Antennas and Propagation (EUCAP)*, Mar. 2012, pp. 1746–1750.

- [40] J. Bechter, F. Roos, and C. Waldschmidt, “Compensation of Motion-Induced Phase Errors in TDM MIMO Radars,” *IEEE Microwave and Wireless Components Letters*, vol. 27, no. 12, pp. 1164–1166, Dec. 2017.
- [41] R. Feger, H. Haderer, and A. Stelzer, “Optimization of Codes and Weighting Functions for Binary Phase-Coded FMCW MIMO Radars,” in *IEEE MTT-S International Conference on Microwaves for Intelligent Mobility (ICMIM)*, May 2016, pp. 1–4.
- [42] W. V. Thillo *et al.*, “Almost perfect auto-correlation sequences for binary phase-modulated continuous wave radar,” in *European Radar Conference*, Oct. 2013, pp. 491–494.
- [43] A. Bourdoux *et al.*, “PMCW Waveform and MIMO Technique for a 79 GHz CMOS Automotive Radar,” in *IEEE Radar Conference (RadarConf)*, May 2016, pp. 1–5.
- [44] A. Vazquez, M. G. Sanchez, I. Cuinas, and M. Dawood, *Wideband Noise Radar based in Phase Coded Sequences, Radar Technology*, G. Kouemou, Ed. InTech, 2010.
- [45] V. Giannini *et al.*, “A 79 GHz Phase-Modulated 4 GHz GHz-BW CW Radar Transmitter in 28 nm CMOS,” *IEEE Journal of Solid-State Circuits*, vol. 49, no. 12, pp. 2925–2937, Dec. 2014.
- [46] D. Guermandi *et al.*, “A 79 GHz Binary Phase-Modulated Continuous-Wave Radar Transceiver with TX-to-RX Spillover Cancellation in 28 nm CMOS,” in *IEEE International Solid-State Circuits Conference*, Feb. 2015, pp. 1–3.
- [47] K. Kobayashi *et al.*, “79 GHz-band Coded Pulse Compression Radar System Performance in Outdoor for Pedestrian Detection,” in *European Radar Conference*, Oct. 2013, pp. 327–330.
- [48] W. V. Thillo *et al.*, “Impact of ADC clipping and quantization on phase-modulated 79 GHz CMOS radar,” in *11th European Radar Conference*, Oct. 2014, pp. 285–288.
- [49] W. Menzel, J. Buechler, and J. Taech, “An Experimental 24 GHz Radar using Phase Modulation Spread Spectrum Techniques,” in *28th European Microwave Conference*, vol. 2, Oct. 1998, pp. 56–60.
- [50] V. Filimon and J. Buechler, “A pre-crash radar sensor system based on pseudo-noise coding,” in *IEEE MTT-S International Microwave Symposium Digest*, vol. 3, Jun. 2000, pp. 1415–1418 vol.3.
- [51] H. J. Ng, R. Feger, and A. Stelzer, “A Fully-Integrated 77-GHz Pseudo-Random Noise Coded Doppler Radar Sensor with Programmable Sequence Generators in SiGe Technology,” in *IEEE MTT-S International Microwave Symposium*, Jun. 2014, pp. 1–4.

- [52] R. Feger, H. Haderer, H. J. Ng, and A. Stelzer, "Realization of a Sliding-Correlator-Based Continuous-Wave Pseudorandom Binary Phase-Coded Radar Operating in W-Band," *IEEE Transactions on Microwave Theory and Techniques*, vol. 64, no. 10, pp. 3302–3318, Oct. 2016.
- [53] H. Haderer, R. Feger, C. Pfeffer, and A. Stelzer, "Millimeter-Wave Phase-Coded CW MIMO Radar Using Zero- and Low-Correlation-Zone Sequence Sets," *IEEE Transactions on Microwave Theory and Techniques*, vol. 64, no. 12, pp. 4312–4323, Dec. 2016.
- [54] T. Hwang *et al.*, "OFDM and Its Wireless Applications: A Survey," *IEEE Transactions on Vehicular Technology*, vol. 58, no. 4, pp. 1673–1694, May 2009.
- [55] R. W. Chang, "Synthesis of Band-Limited Orthogonal Signals for Multichannel Data Transmission," *Bell Syst. Tech. Journal*, vol. 45, no. 10, pp. 1775–1796, 1966.
- [56] S. B. Weinstein and P. M. Ebert, "Data Transmission by Frequency-Division Multiplexing Using the Discrete Fourier Transform," *IEEE Transactions on Communication Technology*, vol. 19, no. 5, pp. 628–634, 1971.
- [57] N. Levanon, "Multifrequency complementary phase-coded radar signal," *IEE Proceedings - Radar, Sonar and Navigation*, vol. 147, no. 6, pp. 276–284, Dec. 2000.
- [58] B. J. Donnet and I. D. Longstaff, "Combining MIMO Radar with OFDM Communications," *Proceedings of the 3rd European Radar Conference*, pp. 37–40, 2007.
- [59] D. Garmatyuk, J. Schuerger, and K. Kauffman, "Multifunctional Software-Defined Radar Sensor and Data Communication System," *IEEE Sensors Journal*, vol. 11, no. 1, pp. 99–106, Jan. 2011.
- [60] C. Sturm and W. Wiesbeck, "Waveform Design and Signal Processing Aspects for Fusion of Wireless Communications and Radar Sensing," *Proceedings of the IEEE*, vol. 99, no. 7, pp. 1236–1259, 2011.
- [61] R. F. Tigrek, W. J. A. De Heij, and P. Van Genderen, "Multi-Carrier Radar Waveform Schemes for Range and Doppler Processing," *IEEE National Radar Conference - Proceedings*, pp. 2–6, 2009.
- [62] C. R. Berger *et al.*, "Signal Processing for Passive Radar Using OFDM Waveforms," *IEEE Journal of Selected Topics in Signal Processing*, vol. 4, no. 1, pp. 226–238, Feb. 2010.
- [63] C. Sturm, E. Pancera, T. Zwick, and W. Wiesbeck, "A Novel Approach to OFDM Radar Processing," in *IEEE National Radar Conference, Proceedings*, no. 3, 2009, pp. 9–12.
- [64] B. Schweizer, C. Knill, D. Schindler, and C. Waldschmidt, "Stepped-Carrier OFDM-Radar Processing Scheme to Retrieve High-Resolution Range-Velocity Profile at

- Low Sampling Rate,” *IEEE Transactions on Microwave Theory and Techniques*, vol. 66, no. 3, pp. 1610–1618, 2017.
- [65] G. Lellouch, A. K. Mishra, and M. Inggs, “Stepped OFDM Radar Technique to Resolve Range and Doppler Simultaneously,” *IEEE Transactions on Aerospace and Electronic Systems*, vol. 51, no. 2, pp. 937–950, 2015.
- [66] C. Pfeffer, R. Feger, and A. Stelzer, “A Stepped-Carrier 77-GHz OFDM MIMO Radar System with 4 GHz Bandwidth,” in *2015 European Radar Conference (EuRAD)*, Sep. 2015, pp. 97–100.
- [67] Z. Wang *et al.*, “Interleaved OFDM Radar Signals for Simultaneous Polarimetric Measurements,” *IEEE Transactions on Aerospace and Electronic Systems*, vol. 48, no. 3, pp. 2085–2099, 2012.
- [68] C. Sturm, Y. L. Sit, M. Braun, and T. Zwick, “Spectrally interleaved multi-carrier signals for radar network applications and multi-input multi-output radar,” *IET Radar, Sonar & Navigation*, vol. 7, no. 3, pp. 261–269, 2013.
- [69] G. M. Brooker, “Mutual Interference of Millimeter-Wave Radar Systems,” *IEEE Transactions on Electromagnetic Compatibility*, vol. 49, no. 1, pp. 170–181, Feb. 2007.
- [70] D. Oprisan and H. Rohling, “Analysis of Mutual Interference between Automotive Radar Systems,” in *International Radar Symposium (IRS)*, 2005, Berlin.
- [71] M. Goppelt, H.-L. Blöcher, and W. Menzel, “Automotive radar - investigation of mutual interference mechanisms,” *Advances in Radio Science*, vol. 8, pp. 55–60, 2010.
- [72] T. Schipper *et al.*, “Discussion of the operating range of frequency modulated radars in the presence of interference,” *International Journal of Microwave and Wireless Technologies*, vol. 6, pp. 371–378, Jun. 2014.
- [73] T. Schipper *et al.*, “An estimation of the operating range for frequency modulated radars in the presence of interference,” in *European Radar Conference (EuRAD)*, Oct. 2013, pp. 227–230.
- [74] G. Hakobyan and B. Yang, “A Novel Narrowband Interference Suppression Method for OFDM Radar,” in *24th European Signal Processing Conference (EUSIPCO)*, Aug. 2016, pp. 2230–2234.
- [75] C. Knill, J. Bechter, and C. Waldschmidt, “Interference of Chirp Sequence Radars by OFDM Radars at 77 GHz,” in *IEEE MTT-S International Conference on Microwaves for Intelligent Mobility (ICMIM)*, Mar. 2017, pp. 147–150.
- [76] C. Fischer, M. Goppelt, H.-L. Blöcher, and J. Dickmann, “Minimizing interference in automotive radar using digital beamforming,” *Advances in Radio Science*, vol. 9, pp. 45–48, 2011.

- [77] C. Fischer, H.-L. Blöcher, J. Dickmann, and W. Menzel, “Robust Detection and Mitigation of Mutual Interference in Automotive Radar,” in *16th International Radar Symposium (IRS)*, Jun. 2015, pp. 143–148.
- [78] M. Barjenbruch *et al.*, “A Method for Interference Cancellation in Automotive Radar,” in *IEEE MTT-S International Conference on Microwaves for Intelligent Mobility (ICMIM)*, Apr. 2015, pp. 1–4.
- [79] S. Heuel, “Automotive Radar Interference Test,” in *18th International Radar Symposium (IRS)*, Jun. 2017, pp. 1–7.
- [80] B. Nuss, L. Sit, and T. Zwick, “A Novel Technique for Interference Mitigation in OFDM Radar Using Compressed Sensing,” in *IEEE MTT-S International Conference on Microwaves for Intelligent Mobility (ICMIM)*, Mar. 2017, pp. 143–146.
- [81] B. E. Tullsson, “Topics in fmcw radar disturbance suppression,” in *Radar 97*, Oct. 1997, pp. 1–5.
- [82] J. Bechter, K. D. Biswas, and C. Waldschmidt, “Estimation and Cancellation of Interferences in Automotive Radar Signals,” in *18th International Radar Symposium (IRS)*, Jun. 2017, pp. 1–10.
- [83] L. Mu, T. Xiangqian, S. Ming, and Y. Jun, “Research on Key Technologies for Collision Avoidance Automotive Radar,” in *Intelligent Vehicles Symposium*, Jun. 2009, pp. 233–236.
- [84] J. Bechter, C. Sippel, and C. Waldschmidt, “Bats-inspired Frequency Hopping for Mitigation of Interference between Automotive Radars,” in *IEEE MTT-S International Conference on Microwaves for Intelligent Mobility (ICMIM)*, May 2016, pp. 1–4.
- [85] J. Bechter, K. Eid, F. Roos, and C. Waldschmidt, “Digital Beamforming to Mitigate Automotive Radar Interference,” in *IEEE MTT-S International Conference on Microwaves for Intelligent Mobility (ICMIM)*, May 2016, pp. 1–4.
- [86] J. Bechter, M. Rameez, and C. Waldschmidt, “Analytical and Experimental Investigations on Mitigation of Interference in a DBF MIMO Radar,” *IEEE Transactions on Microwave Theory and Techniques*, vol. 65, no. 5, pp. 1727–1734, May 2017.